Inorganica Chimica Acta 374 (2011) 163–170

Contents lists available at ScienceDirect

Inorganica Chimica Acta

journal homepage: www.elsevier.com/locate/ica

Sterically crowded triazenides as novel ancillary ligands in copper chemistry

Hyui Sul Lee [a], Mark Niemeyer [b,*]

[a] Institut für Anorganische Chemie, Universität Stuttgart, Pfaffenwaldring 55, D-70569 Stuttgart, Germany
[b] Institut für Anorganische und Analytische Chemie, Johannes-Gutenberg Universität Mainz, Duesbergweg 10-14, D-55128 Mainz, Germany

ARTICLE INFO

Article history:
Available online 3 February 2011

Dedicated to Prof. Kaim

Keywords:
Copper complexes
Sterically crowded ligands
t-Butylisonitrile
Triazenido ligands
Triphenylphosphane

ABSTRACT

We have synthesized copper salts MN_3RR' derived from the biphenyl- or m-terphenyl-substituted triazenes Tph_2N_3H (**1a**) and $Dmp(Tph)N_3H$ (1b) ($Dmp = 2,6\text{-}Mes_2C_6H_3$ with $Mes = 2,4,6\text{-}Me_3C_6H_2$; $Tph = 2\text{-}TripC_6H_4$ with $Trip = 2,4,6\text{-}i\text{-}Pr_3C_6H_2$). The homoleptic copper triazenide $[CuN_3Tph_2]$ (**2a**) was obtained in high yield from the metallation of **1a** with mesityl copper in *n*-heptane, while the complex $[CuN_3(Dmp)Tph]$ (**2b**) was generated by the same method in situ only. Reaction of **2a** with triphenylphosphane gave the 2:1 adduct $[CuN_3Tph_2(PPh_3)_2]$ (**3a**), regardless of the used complex/donor ratio, while reaction of **2a** or **2b** with a stochiometric amount of *t*-butylisonitrile afforded the 1:1 adducts $[Tph_2N_3CuCNtBu]$ (**4a**) and $[Dmp(Tph)N_3CuCNtBu]$ (**4b**). All new compounds (except **2b**) have been characterized by ^1H NMR, ^{13}C NMR and IR spectroscopy, elemental analysis, melting point (not **2a**), and X-ray crystallography. The IR spectroscopic examination of the $\nu(C{\equiv}N)$ stretch in the isonitrile adducts **4a** and **4b** revealed the weaker donor character of the supporting triazenido ligands compared to related β-diketiminato ligands.

1. Introduction

The design and development of alternative ligand systems capable of stabilizing monomeric metal complexes while provoking novel reactivity remains one of the most intensely studied areas of organometallic chemistry [1]. Exploration of this field is driven by the potential use of these complexes in catalysis and organic synthesis. Examples of monoanionic chelating N-donor ligands that have received much recent attention include the β-diketiminate [2] and the amidinate [3] ligand systems. Much less attention has been given to the closely related triazenides [4]. We recently succeeded in the preparation of derivatives of aryl-substituted, sterically crowded triazenido ligands, that are bulky enough to prevent undesirable ligand redistribution reactions [5–7]. These ligands were used to stabilize the first examples of structurally characterized aryl compounds of the heavier alkaline earth metals Ca, Sr, and Ba [5] and unsolvated pentafluorophenyl organyls of the divalent lanthanides Yb and Eu [8]. We have also examined the unusual “inverse” aggregation behavior of alkali metal triazenides in their solid-state structures that can be traced back to a different degree of metal···π-arene interactions to pending aromatic substituents [6]. A series of homologous potassium and thallium complexes crystallizes in isomorphous cells and consists of the first examples of isostructural molecular species reported for these elements [9].

Triazenides are weaker donors than the isoelectronic amidinates and the related β-diketiminates, and should induce greater electrophilicity at a bonded metal atom [5]. In this paper, we describe the synthesis and characterization of several copper triazenides. Isonitrile adducts have been prepared in order to probe the donor properties of our triazenide ligands.

2. Experimental

2.1. Materials and methods

All manipulations were performed by using standard Schlenk techniques under an inert atmosphere of purified argon and solvents freshly distilled from Na wire or $LiAlH_4$. CuMes [10] and the triazenes Tph_2N_3H or $Dmp(Tph)N_3H$ [5,7] were synthesized as previously described. NMR spectra were recorded on Bruker AM200, AC250 or AM400 instruments and referenced to solvent resonances. IR spectra (Nujol mull, CsBr plates) have been obtained in the range 4000–200 cm^{-1} with a Perkin–Elmer paragon 1000 PC spectrometer. Mass spectra were recorded with a Varian MAT711 or Finnegan MAT95 instrument. Melting points were determined under Ar atmosphere in sealed glass tubes.

2.2. Preparation of $[CuN_3Tph_2]$ (**2a**)

A solution of CuMes (0.365 g, 2 mmol) and triazene **1a** (1.204 g, 2 mmol) in *n*-heptane (60 mL) was stirred for 2 h. The volume was reduced to ca. 30 mL under vacuum and the obtained precipitate

---

* Corresponding author. Tel.: +49 6131 39 26020; fax: +49 6131 39 25419.
E-mail address: niemeyer@uni-mainz.de (M. Niemeyer).

0020-1693/$ - see front matter © 2011 Elsevier B.V. All rights reserved.
doi:10.1016/j.ica.2011.01.079

was redissolved by slight warming. Storage at ambient temperature for two days afforded **2a** as yellow crystalline material. Yield: 0.90 g (1.35 mmol, 76%); ^1H NMR (250.1 MHz, C_6D_6): δ 0.96 (d, $^3J_{HH}$ = 6.9 Hz, 12H, o-$CH(CH_3)_2$), 1.04 (d, $^3J_{HH}$ = 6.9 Hz, 12H, o-$CH(CH_3)_2$), 1.41 (d, $^3J_{HH}$ = 6.9 Hz, 12H, p-$CH(CH_3)_2$), 2.78 (sep, $^3J_{HH}$ = 6.9 Hz, 4H, o-$CH(CH_3)_2$), 2.98 (sep, $^3J_{HH}$ = 6.9 Hz, 2H, p-$CH(CH_3)_2$), 7.27 (s, 4H, m-Trip), 7.13 (t, 2H, 5-C_6H_4), 6.99 (d, $^3J_{HH}$ = 7.9 Hz, 2H, 3-C_6H_4), 6.93 (t, $^3J_{HH}$ = 7.3 Hz, 2H, 4-C_6H_4), 5.99 (d, $^3J_{HH}$ = 8.0 Hz, 2H, 6-C_6H_4). ^{13}C NMR (100.6 MHz, C_6D_6): δ 23.5 (o-$CH(CH_3)_2$), 24.5 (p-$CH(CH_3)_2$), 24.7 (o-$CH(CH_3)_2$), 30.8 (o-$CH(CH_3)_2$), 35.0 (p-$CH(CH_3)_2$), 121.9 (m-Trip), 124.9 (4-C_6H_4), 125.8 (6-C_6H_4), 128.2 (5-C_6H_4), 132.3 (3-C_6H_4), 132.8 (2-C_6H_4), 135.3 (i-Trip), 146.8 (o-Trip), 148.1, 148.8 (1-C_6H_4, p-Trip). IR (Nujol) $\tilde{\nu}$ = 1606 m, 1571 m, 1567 m, 1488 sh, 1361 s, 1338 vs, 1334 vs, 1284 s, 1250 m, 1241 m, 1184 m, 1168 m, 1157 m, 1127 w, 1103 m, 1069 m, 1055 m, 1003 m, 939 m, 877 ms, 780 w, 774 s, 760 vs, 753 vs, 722 m, 670 w, 626 w, 520 w 477 w, 422 m. *Anal.* Calc. for $C_{42}H_{54}CuN_3$: C, 75.92; H, 8.19; N, 6.32. Found: C, 76.12; H, 8.33; N 6.13%.

2.3. Preparation of [$CuN_3Tph_2(PPh_3)_2$] (**3a**)

PPh_3 (1.05 g, 4.00 mmol) was added at ambient temperature to a stirred solution of **2a** (2.00 mmol) in toluene (60 mL). After 2 h the solvent was removed under reduced pressure and the remaining solid was dissolved in a *n*-heptane/toluene mixture. Storage at 0 °C for several days afforded **3a** $\mathbf{C_7H_8}$ as pale yellow crystalline material. The solvent-free complex **3a** was obtained by thoroughly drying under vacuum. Yield: 1.75 g (1.47 mmol, 74%); mp: 185–190 °C; ^1H NMR (250.1 MHz, C_6D_6): δ 0.93 (d, $^3J_{HH}$ = 6.8 Hz, 12H, o-$CH(CH_3)_2$), 1.14 (d, $^3J_{HH}$ = 6.8 Hz, 12H, o-$CH(CH_3)_2$), 1.25 (d, $^3J_{HH}$ = 6.8 Hz, 12H, p-$CH(CH_3)_2$), 2.86 (sep, $^3J_{HH}$ = 6.7 Hz, 2H, p-$CH(CH_3)_2$), 2.93 (sep, $^3J_{HH}$ = 6.9 Hz, 4H, o-$CH(CH_3)_2$), 6.55 (d, $^3J_{HH}$ = 7.8 Hz, 2H, 6-C_6H_4), 6.93–7.03 (m, 32H, PPh_3 + 3-C_6H_4), 6.89 (t, $^3J_{HH}$ = 7.0 Hz, 2H, 4-C_6H_4), 7.12 (t, 2H, 5-C_6H_4), 7.14 (s, 4H, m-Trip). ^{13}C NMR (100.6 MHz, C_6D_6): δ 24.1 (o-$CH(CH_3)_2$), 24.5 (p-$CH(CH_3)_2$), 25.0 (o-$CH(CH_3)_2$), 31.1 (o-$CH(CH_3)_2$), 34.6 (p-$CH(CH_3)_2$), 120.9 (m-Trip), 121.0 (4-C_6H_4), 123.0 (6-C_6H_4), 127.2 (5-C_6H_4), 128.7 (d, $^3J_{PC}$ = 8.4 Hz, m-PPh_3), 129.5 (d, $^4J_{PC}$ = 0.5 Hz, p-PPh_3), 130.7 (2-C_6H_4), 132.8 (3-C_6H_4), 134.4 (d, $^2J_{PC}$ = 16.5 Hz, o-PPh_3), 135.0 (d, $^1J_{PC}$ = 15.2 Hz, i-PPh_3), 139.1 (i-Trip), 146.5 (o-Trip), 146.5 (p-Trip), 150.8 (1-C_6H_4); ^{31}P NMR (162.0 MHz, C_6D_6): δ −1.9; IR (Nujol) $\tilde{\nu}$ = 1604 w, 1556 s, 1530 ms, 1478 ms, 1455 ms, 1359 s, 1339s, 1249 s, 1202 ms, 1156 m, 1093 ms, 1069 s, 1057 w, 1001 m, 968 w, 942 m, 920 w, 895 w, 878 m, 873 m, 850 w, 845 s, 779 w, 784 w, 769 m, 756 s, 743 vs, 729 s, 704 s, 694 vs, 660 m, 649 ms, 590 w, 556 w, 527 ms, 501 vs, 464 m, 439 w. *Anal.* Calc. for $C_{78}H_{84}CuN_3P_2$: C, 78.79; H, 7.12; N, 3.53. Found: C, 78.62; H, 7.30; N 3.49%.

2.4. Preparation of [$Tph_2N_3CuCN^tBu$] (**4a**)

^{t}BuNC (0.23 mL, 2 mmol) was added to a stirred solution of **1a** (1.20 g, 2 mmol) in *n*-heptane (50 mL). The volume of the resulting yellow solution was reduced to incipient crystallization under reduced pressure. Storage at ambient temperature overnight afforded **4a** as pale yellow crystals. The workup of the mother liquor gave another crop of crystalline material. Yield: 1.07 g (1.43 mmol, 72%); mp: 210–214 °C; ^1H NMR (400.1 MHz, C_6D_6): δ 0.83 (s, 9H, $C(CH_3)_3$), 1.17 (d, $^3J_{HH}$ = 6.8 Hz, 12H, o-$CH(CH_3)_2$), 1.19 (d, $^3J_{HH}$ = 6.8 Hz, 12H, o-$CH(CH_3)_2$), 1.27 (d, $^3J_{HH}$ = 6.8 Hz, 12H, p-$CH(CH_3)_2$), 2.82 (sep, $^3J_{HH}$ = 6.9 Hz, 2H, p-$CH(CH_3)_2$), 3.03 (sep, $^3J_{HH}$ = 6.9 Hz, 2H, o-$CH(CH_3)_2$), 6.99 (t, $^3J_{HH}$ = 7.2 Hz, 2H, 5-C_6H_4), 7.10 (d, $^3J_{HH}$ = 7.5 Hz, 2H, 3-C_6H_4), 7.13 (s, 4H, m-Trip), 7.30 (t, $^3J_{HH}$ = 7.6 Hz, 2H, 4-C_6H_4), 7.96 (d br, $^3J_{HH}$ = 7.6 Hz, 2H, 6-C_6H_4). ^{13}C NMR (100.6 MHz, C_6D_6): δ 24.5, 24.5, 24.9 (2 × o-$CH(CH_3)_2$, p-$CH(CH_3)_2$), 29.5 ($C(CH_3)_3$), 30.9 (o-$CH(CH_3)_2$), 34.6 (p-$CH(CH_3)_2$), 119.0 (6-C_6H_4), 120.9 (m-Trip), 122.0 (4-C_6H_4), 128.4 (5-C_6H_4), 130.7 (i-Trip), 131.3 (3-C_6H_4), 147.1 ($CNC(CH_3)_3$), 147.3 (o-Trip), 147.3 (p-Trip), 151.0 (1-C_6H_4); signals for the $CNC(CH_3)_3$ $CNC(CH_3)_3$ and 2-C_6H_4 carbon atoms could not be detected. IR (Nujol) $\tilde{\nu}$ = 2198 s ($\tilde{\nu}_{CN}$), 1604 m, 1592 m, 1585 sh, 1567 m, 1508 m, 1484 sh, 1361 s, 1336 s, 1308 s br, 1242 vs br, 1193 s, 1158 ms, 1128 m, 1102 m, 1069 m, 1056 m, 1004 m, 953 w, 938 m, 919 w, 882 sh, 875 ms, 774 m, 756 vs, 727 ms, 693 w, 654 ms, 591 w, 555 w, 484 w. *Anal.* Calc. for $C_{47}H_{63}CuN_4$: C, 75.51; H, 8.49; N, 7.49. Found: C, 75.42; H, 8.35; N 7.43%.

2.5. Preparation of [$Dmp(Tph)N_3CuCN^tBu$] (**4b**) and **4b** · $\mathbf{C_6H_6}$

A solution of the triazene $Dmp(Tph)N_3H$ (1.27 g, 2 mmol) and CuMes (0.365 g, 2 mmol) in 40 mL of *n*-heptane was stirred for 2 h. ^{t}BuNC (0.23 mL, 2 mmol) was added and stirring was continued overnight. The volume of the resulting yellow solution was reduced to incipient crystallization under reduced pressure. Storage at ambient temperature for several days afforded **4b** as light yellow crystals. Yield: 0.84 g (0.97 mmol, 49%). mp: 186–194 °C; ^1H NMR (200.1 MHz, C_6D_6): δ 0.86 (s, 9H, $C(CH_3)_3$), 1.01 (d, $^3J_{HH}$ = 7.0 Hz, 6H, o-$CH(CH_3)_2$), 1.04 (d, $^3J_{HH}$ = 6.9 Hz, 6H, o-$CH(CH_3)_2$), 1.22 (d, $^3J_{HH}$ = 6.9 Hz, 6H, p-$CH(CH_3)_2$), 2.24 (s, 6H, p-CH_3), 2.27 (s, 12H, o-CH_3), 2.76 (sept, $^3J_{HH}$ = 6.9 Hz, 2H, o-$CH(CH_3)_2$), 2.76 (sept, $^3J_{HH}$ = 6.9 Hz, 1H, p-$CH(CH_3)_2$), 6.88 (s, 4H, m-Mes), 6.70–7.25 (m, 7H, Aryl-H), 7.00 (s, 2H, m-Trip). ^{13}C NMR (62.9 MHz, C_6D_6): δ 21.2 (p-CH_3), 21.4 (o-CH_3), 24.5 (p-$CH(CH_3)_2$), 24.5 (o-$CH(CH_3)_2$), 25.0 (o-$CH(CH_3)_2$), 29.5 ($NC(CH_3)_3$), 30.6 (o-$CH(CH_3)_2$), 34.6 (p-$CH(CH_3)_2$), 55.9 ($NC(CH_3)_3$), 118.0, 120.8, 123.5, 128.0, 130.5 (various aromatic CH), 120.8 (m-Trip), 128.2 (m-Mes), 129.8 (m-C_6H_3), 128.8, 133.9, 134.9, 135.6, 135.8, 140.1, 146.9, 147,2 147,6 149.7 (various aromatic C); one signal for the $CNC(CH_3)_3$ carbon atom could not be detected. IR (Nujol) $\tilde{\nu}$ = 2193 s ($\tilde{\nu}_{CN}$), 1588 m, 1566 m, 1556 sh, 1536 s, 1530 s, 1500 sh, 1461 vs, 1415 m, 1378 vs, 1360 sh, 1306 m, 1275 ms, 1262 s, 1242 m, 1229 m, 1206 m, 1189 ms, 1167 s, 1069 sh, 1030 vw, 1001 w, 938 sh, 978 w, 785 m, 777 w, 754 vs, 739 ms, 724 ms, 695 m, 654 m, 600 w, 591 w, 575 w, 546 w, 515w. *Anal.* Calc. for $C_{50}H_{61}CuN_4$: C, 76.84; H, 7.87; N, 7.17. Found: C, 76.90; H, 7.65; N 7.06%. Crystals of the packing complex **4b**·$\mathbf{C_6H_6}$ were grown from a saturated benzene solution.

2.6. X-ray crystallography

X-ray-quality crystals were obtained as described in the experimental section. Crystals were removed from Schlenk tubes and immediately covered with a layer of viscous hydrocarbon oil (Paratone N, Exxon). A suitable crystal was selected, attached to a glass fiber, and instantly placed in a low-temperature N_2-stream [11a]. All data were collected at 100 K (**2a**, **4b**, **4b**·(C_6H_6)) or 173 K (**1a**, **3a**, **4b**) using either a Siemens P4 (**3a**), a rebuild Syntex $P2_1$/Siemens P3 (**3a**, **4b**) or a Nonius Kappa CCD (**2a**, **4b**, **4b**·(C_6H_6)) diffractometer. Crystal data are given in Table 1. Calculations were performed with the SHELXTL PC 5.03 [11b] and SHELXL-97 [11c] program system installed on a local PC. The structures were solved by direct methods and refined on F_o^2 by full-matrix least-squares refinement. Absorption corrections were applied by using semiempirical ψ-scans or a multi-scan refinement. Anisotropic thermal parameters were included for all non-hydrogen atoms. In **1a** the methyl carbon atoms of two disordered iso-propyl groups were refined with split positions and side occupation factors of 0.50 for C242, C243/C244, C245 and C442, C443/C444, C445. The corresponding C241–C242, C241–C243, C241–C244, C241–C245, C441–C442, C441–C443, C441–C444 and C441–C445 distances were restrained with DFIX commands. In **3a** the ring carbon atoms

Table 1
Selected crystallographic data for compounds **1a**, (**2a**)$_2$, **3a·C$_7$H$_8$**, **4b**, and **4b·C$_6$H$_6$**.[a]

	1a	(**2a**)$_2$	**3a·C$_7$H$_8$**	**4b·C$_6$H$_6$**	**4b** (100 K)	**4b** (173 K)
Formula	$C_{42}H_{55}N_3$	$C_{84}H_{108}Cu_2N_6$	$C_{85}H_{92}CuN_3P_2$	$C_{56}H_{67}CuN_4$	$C_{50}H_{61}CuN_4$	$C_{50}H_{61}CuN_4$
Molecular mass	601.89	1328.84	1281.10	859.68	781.57	781.57
Color, habit	pale yellow, prism	pale yellow, plate	pale yellow, plate	yellow, prism	yellow, prism	yellow, prism
Crystal size (mm)	0.80 × 0.40 × 0.40	0.30 × 0.20 × 0.04	0.80 × 0.50 × 0.20	0.25 × 0.25 × 0.20	0.40 × 0.35 × 0.25	0.65 × 0.55 × 0.45
Crystal system	monoclinic	tetragonal	triclinic	monoclinic	triclinic	triclinic
Space group	$C2/c$	$P4_3$	$P\bar{1}$	$P2_1/c$	$P\bar{1}$	$P\bar{1}$
a (Å)	33.037(7)	15.0461(1)	13.601(3)	17.6453(2)	10.6956(2)	10.752(2)
b (Å)	9.6910(19)	15.0461(1)	14.059(3)	12.2230(2)	12.2829(2)	12.311(3)
c (Å)	25.009(5)	33.6042(4)	19.314(5)	22.6382(3)	19.1514(3)	19.281(4)
α (°)	90	90	80.956(18)	90	72.0978(10)	71.992(16)
β (°)	106.99(3)	90	85.469(17)	94.4469(7)	89.1996(11)	88.779(17)
γ (°)	90	90	89.487(19)	90	70.2091(10)	70.314(16)
V (Å^3)	7657(3)	7607.49(12)	3635.8(14)	4867.87(12)	2241.31(7)	2275.5(8)
Z	8	4	2	4	2	2
D_{calc} (g/cm^3)	1.044	1.160	1.170	1.173	1.158	1.141
μ (mm^{-1})	0.060	0.605	0.390	0.488	0.524	0.516
2θ Range (°)	3.4–52.0	6.5–56.6	4.2–50.0	6.6–56.5	7.1–56.6	3.6–48.0
Collected data	7688	45 928	13 238	65 762	66 066	7581
Unique data/$R_{(int)}$	7500/0.042	16 606/0.091	12 656/0.035	11 972/0.090	11 049/0.158	7145/0.069
Data with $I > 2\sigma(I)$ (N_o)	4635	14 009	7965	10 115	9314	4902
Number of parameters (N_p)	467	853	825	600	525	525
Number of restraints	8	1	0	0	0	0
R_1 ($I > 2\sigma(I)$)[b]	0.070	0.052	0.046	0.050	0.055	0.068
wR_2 (all data)[c]	0.181	0.110	0.113	0.106	0.162	0.187
Goodness-of-fit GOF[d]	1.409	1.234	0.860	1.045	1.682	1.119
Difference e$^-$ density (e Å^3)	0.38/−0.26	0.43/−0.43	0.68/−0.43	0.31/−0.40	0.53/−1.05	0.33/−0.77

[a] All data were collected at 173 K (**1a**, **3a·C$_7$H$_8$**, **4b**) or 100 K (**2a**, **4b**, **4b · C$_6$H$_6$**), using Mo Kα (= 0.71073 Å) radiation.
[b] $R_1 = \Sigma(||F_o| - |F_c||)/\Sigma(|F_o|$.
[c] $wR_2 = \{\Sigma[w(F_o^2 - F_c^2)^2]/\Sigma[w(F_o^2)^2]\}^{1/2}$.
[d] $\mathrm{GOF} = \{\Sigma[w(F_o^2 - F_c^2)^2]/(N_o - N_p)\}^{1/2}$.

of a cocrystallized toluene molecule were constrained to a regular hexagon. In the structure determination of **4b**, obtained at 100 K (173 K), the copper atom was refined with split positions and temperature-dependent side occupation factors of 0.95 (0.88) and 0.05 (0.12) that correspond to different η^1-N3 and η^2-N1,N3 coordination modes, respectively (see supporting information). In **4b**·(C$_6$H$_6$) the carbon atoms of the cocrystallized, rotationally disordered benzene ring (sof = 0.5 for C71–C76/C81–C86) were constrained to regular hexagons. Final *R* values are listed in Table 1. Important bond parameters are given in in Table 2. Further details are provided in the supplementary material.

3. Results and discussion

3.1. Syntheses and characterization of the triazene HN_3Tph_2

As we and others have reported before [5–7,9,12], bulky substituted diaryl triazenes are accessible in high yields by the reaction of lithium aryls with aryl azides followed by a protolytic workup. Since we have given only limited information for the bis(biphenyl) substituted triazene HN_3Tph_2 in a preliminary communication [6] some more details including the crystal structure will be provided in the following section.

After crystallization from acetone, triazene **1a** is obtained as pale yellow solid in 75% yield. The air stable but acid labile compound melts with slight decomposition in the range 190–195 °C. In the IR spectrum the asymmetric *N*–*N*=N and N–*N*=*N* vibrations at 1510 cm^{-1} and 1149 cm^{-1} indicate a mainly localized π-electron system. The NH-stretch is observed as a narrow band at 3300 cm^{-1}. The ^{1}H and ^{13}C NMR spectra show only one set of signals and therefore indicate that only one of several possible isomers (Scheme 1) dominates in solution.

The triazene crystallizes as a monomer in the space group *C*2/*c* (Fig. 1). Further aggregation involving intermolecular N–H···A hydrogen bridges (A = N, O, and Br) as often observed in other 1,3-disubstituted triazenes [14,15] is prohibited by the sterically crowded Tph substituents. **1a** possesses a trans-conformation around the central N=N double bond as shown by the torsion angles C11–N1–N2–N3 [−175.7(2)°] and H3–N3–N2–N1 [0(2)°] and therefore exists as E-anti isomer according to the nomenclature of scheme 1. In addition, the torsion angles N2–N1–C11–C16 [−1.4(3)°] and N2–N3–C31–C36 [−3.2(3)°] indicate a syn/syn arrangement of the Tph substituents that point in direction of the NH hydrogen atom. With interplanar angles of 78.7° and 76.9° the Trip groups are aligned almost orthogonal to the C_6H_4 arene rings with a staggered conformation of the iso-propyl substituents (Fig. 1, right).

The difference between the N=N (1.280(3) Å for N1–N2) and N–N (1.318(3) Å for N2–N3) bond lenghts is less as one might expect for localized bonds. Bigger differences of 1.2650(15)/1.3525(15) Å are observed in the solid state structure of the terphenyl substituted triazene $HN_3(Me_4Ter)_2$ (Me_4Ter = 3,5,3″,5″-tetramethyl-1,1′:3′,1″-terphenyl-2′) [7]. The more delocalized bonds in **1a** may be explained in part by the coplanar arrangement of the $(C_6H_4)N_3(C_6H_4)$ fragments, since for the triazene $HN_3(Me_4Ter)_2$ a bigger torsion for the aryl substituents is found, as shown by the NNCC dihedral angles of 43.5°/53.8°. However, another part of the more balanced bonds in **1a** may be due to disorder since the NH positions on N3 and N1 are populated with 75% and 25%, respectively (see Supporting information).

3.2. Syntheses of copper triazenides

Donor-free copper triazenides are accessible in n-heptane as the solvent via metallation of the diaryltriazenes Tph_2N_3H (**1a**) or $Dmp(Tph)N_3H$ (**1b**) (Dmp = 2,6-$Mes_2C_6H_3$ with Mes = 2,4,6-$Me_3C_6H_2$; Tph = 2-$TripC_6H_4$ with Trip = 2,4,6-$^iPr_3C_6H_2$) with mesityl copper (Scheme 2).

After crystallization, the pale yellow complex $[Cu(N_3Tph_2)]$ (**2a**) was isolated in 76% yield, whereas the complex

Table 2
Selected bond distances (Å), angles (°), and dihedral angles (°) for Compounds **1a**, **2a**, **3a**·C_7H_8, **4b**, and **4b**·C_6H_6.

1a	
N1–N2	1.280(3)
N2–N3	1.319(3)
N3–H3	0.87(3)
N1–C11	1.417(3)
N3–C31	1.398(3)
N1–N2–N3	110.63(19)
N2–N1–C11–C16	−1.4(3)
N2–N3–C31–C36	−3.2(3)
*(**2a**)$_2$*	
Cu1–N1	1.878(2)
Cu2–N3	1.887(2)
Cu1–N4	1.885(2)
Cu2–N6	1.878(3)
Cu1···Cu2	2.4765(5)
N1–N2	1.311(3)
N2–N3	1.306(3)
N4–N5	1.316(3)
N5–N6	1.302(3)
N3–N2–N1	115.9(2)
N6–N5–N4	115.9(2)
N2–N1–C11–C16	−140.7(3)
N2–N3–C31–C36	−141.2(3)
N5–N4–C51–C56	−55.8(4)
***3a**·C_7H_8*	
Cu–N1	2.220(2)
Cu–N3	2.117(2)
Cu–P1	2.2706(9)
Cu–P2	2.2814(9)
N1–N2	1.315(3)
N2–N3	1.309(3)
N1–C11	1.419(3)
N3–C31	1.418(3)
N3–N2–N1	109.2(2)
N3–Cu–N1	59.06(8)
P1–Cu–P2	121.61(3)
P1–Cu···N2	122.3(5)
P2–Cu···N2	114.8(5)
N2–N1–C11–C16	−31.2(3)
N2–N3–C31–C36	−165.8(2)
***4b**·C_6H_6*	
Cu–N3	1.8948(12)
Cu–C1	1.8337(15)
N1–N2	1.2816(16)
N2–N3	1.3354(16)
N1–C11	1.4189(18)
N3–C31	1.3968(17)
C1–N5	1.147(2)
C1–Cu–N3	173.73(5)
N1–N2–N3	110.60(11)
N2–N3–Cu	117.30(9)
C31–N3–Cu	127.97(9)
N5–C1–Cu	176.86(13)
N2–N1–C11–C16	−42.77(17)
N2–N3–C31–C36	21.64(17)
***4b** at −173 °C*	
Cu1–N3	1.8934(14)
Cu1–C1	1.829(2)
Cu2–N1	1.972(6)
Cu2–N3	2.073(7)
N1–N2	1.2829(19)
N2–N3	1.3328(19)
N2–N1–C11–C16	−37.3(2)
N2–N3–C31–C36	12.8(2)
***4b** at −100 °C*	
Cu1–N3	1.900(3)
Cu1–C1	1.834(4)
Cu2–N1	1.914(5)
Cu2–N3	2.283(7)
N1–N2	1.285(4)
N2–N3	1.325(4)
N2–N1–C11–C16	−36.5(5)
N2–N3–C31–C36	12.6(5)

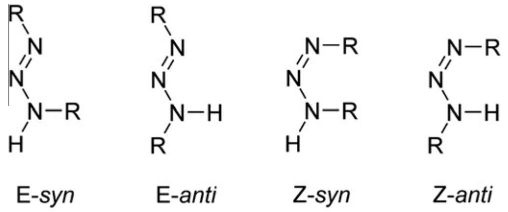

Scheme 1. Possible isomers of triazenes according to the nomenclature of amidinates [13].

$[Cu(N_3(Dmp)Tph_2)]$ (**2b**) was generated in situ only. Reaction of **2a** or **2b** with a stochiometric amount of *t*-butylisonitrile afforded the 1:1 adducts $[Tph_2N_3CuCN^tBu]$ (**4a**) and $[Dmp(Tph)N_3CuCN^tBu]$ (**4b**). However, reaction of **2a** with triphenylphosphane gave the 2:1 adduct $[CuN_3Tph_2(PPh_3)_2]$ (**3a**), regardless of the used complex/donor ratio. The donor-free complex **2a** is oxygen and air-sensitive whereas the adducts are air-stable in the solid-state for days. All compounds possess good or moderate solubility in aromatic or aliphatic hydrocarbons. They show considerable thermal stability but decompose with N_2 evolution at higher temperature (**3a**: 185–190 °C, **4a**: 210–214 °C, **4b**: 186–194 °C).

3.3. IR spectroscopic characterization of copper triazenides

The most important bonding modes in metal triazenides are shown in Scheme 3. IR spectroscopy should be in principle a valuable tool for the assignment of different coordination modes as was already stated by Moore and Robinson in an older review on the coordination chemistry of triazenides [4a].

However, due to the lack of structually characterized compounds these assignments have been ambigous for some time. In the meantime we and others have synthesized numerous metal triazenides that have been characterized by IR spectroscopy and X-ray crystallography. Table 3 summarizes characteristic IR vibrations together with the corresponding bonding modes as determined by X-ray structure determinations in our group.

A broad intense ν_{as}-N_3 absorption in the range 1221–1282 cm^{-1} as observed for the monomeric complexes $[M(N_3Tph_2)]$ {M = (thf)Li, Na, [17], K [6], Rb [17], Cs [6], Tl [9], Me_2Al [18], $(Ph_3P)_2Cu$ (**4a**), $(C_5H_4Me)_2Er$ [17]} indicates an η^2-chelating bonding mode of the triazenido ligand. An η^1-coordination mode, as found in several halogeno mercury triazenides [16], is accompanied by two intense bands in the range 1306–1317 cm^{-1} and 1163–1178 cm^{-1}. In complexes that have a shallow energy profile for the coordination of the metal cations as indicated by disorder in the X-ray structures (e.g. $[Cu\{N_3(Dmp)Tph\}(CNtBu)]$ (**4b**) and $[ZnR(N_3Tph_2)]$ (R = Me, Et [17]) superpositions of the corresponding η^1- and η^2-typical vibration patterns are observed. The IR spectroscopic characterization of the complex $[Cu(N_3Tph_2)(CNtBu)]$ (**4a**), which could not be structurally authenticated by X-ray diffraction, shows the population of both η^1 and η^2 bonding modes.

The symmetrically $\mu,\eta^1\eta^1$-bridged copper complex $[Cu(N_3Tph_2)]_2$ (**2a**)$_2$ possesses an intense broad ν_{as}-N_3 vibration at 1334 cm^{-1}. A corresponding, although less intense absorption at 1336 cm^{-1} and further bands typical for the other coordination modes are observed at 1309/1243/1167 cm^{-1} for the unsymmetrically $\mu,\eta^1\eta^2$-bridged lithium complex $[Li(N_3Tph_2)]_2$ [6].

With the prepared isonitrile adducts **4a** and **4b** it is possible to examine the donor character of the triazenido ligands experimentally. Thereby, the $\nu(C{\equiv}N)$ vibration of the isonitrile ligand is used as an IR spectroscopic probe. Table 4 shows a comparison of the corresponding absorption bands in copper complexes with different monoanionic N-donor ligands. The observed vibrations of

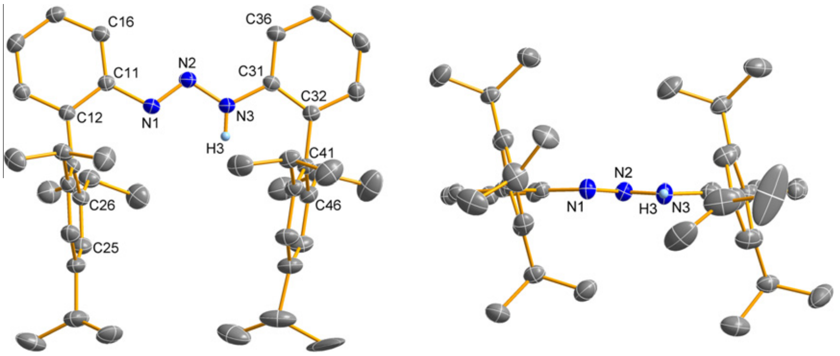

Fig. 1. Molecular structure of **1a** with thermal ellipsoids set to 30% probability. Hydrogen atoms with exception of the N–H one have been omitted for clarity.

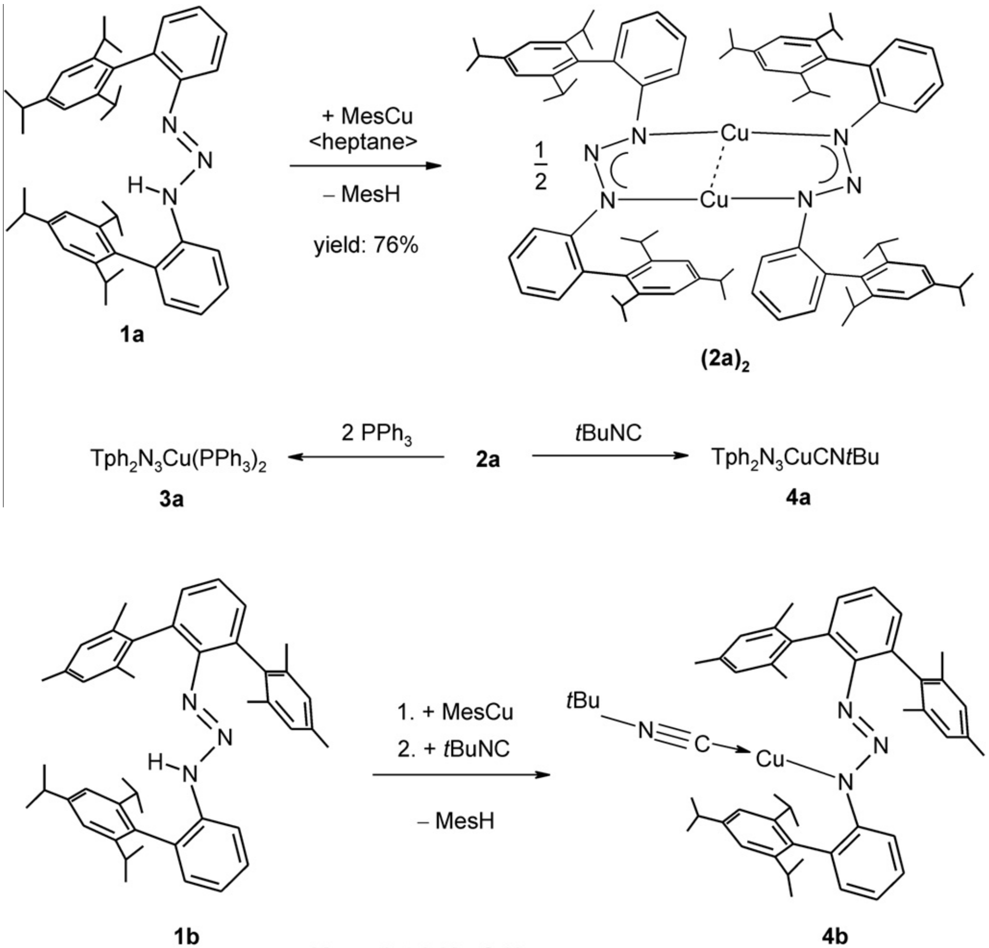

Mes = 2,4,6-$Me_3C_6H_2$

Tph = 2-TripC_6H_4 with Trip = 2,4,6-$iPr_3C_6H_2$

Scheme 2. Synthesis of compounds **2a–4b**.

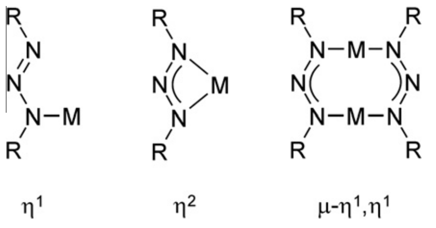

Scheme 3. Important bonding modes in metal triazenides.

2199 cm^{-1} (**4a**) and 2193 cm^{-1} (**4b**) are shifted to higher wave numbers than the corresponding values in copper β-diketiminates (2121–2148 cm^{-1}) [20a–c,20e] or in a copper tris(pyrazolyl)borate (2155 cm^{-1}) [20f]. However, a similar high value of 2196 cm^{-1} is found for a copper complex with an electron-deficient trifluoromethyl-substituted tris(pyrazolyl)borate ligand [20g] while a copper triazapentadienide shows an absorption at 2176 cm^{-1} [20e]. In the three-nuclear pyrazolato complex [(CO)$_3$Re(pz)$_3${Cu(CNc-Hex)}$_2$] [20h], which possesses two different binding modes, two vibrations at 2164 cm^{-1} and 2210 cm^{-1} are observed that can be

Table 3
Selected IR spectroscopic data for metal triazenides.

Formula	Bonding mode[a]	Characteristic NNN vibrations (cm^{-1})[b]	References
$[Cl{-}Hg\{N_3(Dmp)Mph\}]$	η^1	$\underline{1314}$, $\underline{1163}$	[16]
$[I{-}Hg\{N_3(Dmp)Mph\}]$	η^1	$\underline{1316}$ br, $\underline{1169}$ br	[16]
$[I{-}Hg\{N_3(Dmp)Tph\}]$	η^1	1313, 1166 br	[16]
$[Cu(N_3Tph_2)(PPh_3)_2]$ (**3a**)	η^2	1246 br	this work
$[Na(N_3Tph_2)]$	η^2	1305, $\underline{1242{-}1227}$ br	[17]
$[K(N_3Tph_2)]$	η^2	1298, $\underline{1236}$ br	[6]
$[Rb(N_3Tph_2)]$	η^2	1225 br	[17]
$[Cs(N_3Tph_2)]$	η^2	1221 br	[6]
$[Li(N_3Tph_2)(thf)]$	η^2	1243 br	[17]
$[Tl(N_3Tph_2)]$	η^2	1300, $\underline{1248}$ br	[9]
$[AlMe_2(N_3Tph_2)]$	η^2	1282 br	[18]
$[Er(C_5H_4Me)_2N_3Tph_2]$	η^2	1247 br	[17]
$[Eu\{N_3(Dmp)Tph\}_2]$	η^2	1283 br	[19]
$[Cu(N_3Tph_2)(CNtBu)]$ (**4a**)	unknown	1317, 1266–1233, $\underline{1178}$	this work
$[Cu\{N_3(Dmp)Tph\}(CNtBu)]$ (**4b**)	$\eta^1 + \eta^2$	1306, $\underline{1262}$ br, $\underline{1167}$ br	this work
$[ZnMe(N_3Tph_2)]$	$\eta^1 + \eta^2$	$\underline{1310{-}1240}$ br, 1169	[17]
$[ZnEt(N_3Tph_2)]$	$\eta^1 + \eta^2$	$\underline{1306{-}1260}$ br, 1168	[17]
$[Cu(N_3Tph_2)]_2$ (**2a**)$_2$	$\mu, \eta^1/\eta^1$	1334 br	this work
$[Li(N_3Tph_2)]_2$	$\mu, \eta^1/\eta^2$	1336, 1309, $\underline{1243}$ br, 1167	[6]

[a] As verified by X-ray diffraction.

[b] If more than one characteristic NNN vibration is present the most intense is underlined.

assigned to the three- and two-coordinate copper atoms, respectively. Therefore, these results clearly support the predicted weaker donor character of triazenides compared to β-diketiminates. Unfortunately, comparable data for copper amidinates have not been reported yet.

3.4. Structural studies of copper triazenides

Crystals suitable for X-ray diffraction experiments could be obtained from *n*-heptane or *n*-heptane/toluene mixtures with exception of the isonitrile adduct **4a**. For **5a** co-crystallization of the used solvent was observed. Since the structure refinement of complex **4b** gave only poor results due to disorder of the copper atom, the compound was recrystallized from benzene to give the packing complex **4b**·C_6H_6. Figs. 2–5 show the molecular structures of the examined complexes, important bond parameters are summarized in Table 3.

3.4.1. Molecular structure of the homoleptic copper triazenide $[CuN_3Tph_2]$ (**2a**)

The complex crystallizes as dimers without additional imposed symmetry in the tetragonal space group $P4_3$ (Fig. 2). In the dimeric units both two-coordinate metal atoms are bridged by two triazenido ligands in a $\mu,\eta^1\eta^1$-fashion. The slight deviation from an almost linear coordination (N1–Cu1–N4: 169.36(11), N3–Cu2–N6: 169.18(11)) may be attributed to the presence of small-bite ligands that causes Pauli repulsion between the metal centers. A nearly realized C_2-symmetry with a twofold axis perpendicular to the Cu_2N_3 plane is broken by small but significant differences in the conformation of the Tph substituents. The central Cu_2N_6 fragment is not planar and both N_3 planes are tilted by 29.8° to each other (Fig. 2, right). The copper atoms Cu1/Cu2 are displaced by 0.213 Å/−0.395 Å and −0.411 Å/0.185 Å from the planes defined by the nitrogen atoms N1N2N3 and N4N5N6 and the Tph substituents alternately point above and below the central eight-membered ring. Therefore, a syn/anti-conformation of the respective triazenido ligands with torsion angles N–N–Cn1–Cn6 of approximately −55° and −141° is observed. Within the Tph- substituents the arene rings of the C_6H_4 and Trip fragments possess an almost orthogonal alignment with interplanar angles of 63.9° (C1n/C2n), 75.8° (C3n/C4n), 76.2° (C5n/C6n) and 68.8° (C7n/C8n).

Table 4
$\nu(C{\equiv}N)$-vibrations in isonitrile adducts of copper complexes with different monoanionic N-donor ligands.

$\nu(C{\equiv}N)$ (cm^{-1})	Compounds	References
2121	$[C\{C(Me)N(Mes)\}_2]Cu(CNXyl)$	[20a]
2126	$[C\{C(Me)N(Dip)\}_2]Cu(CNXyl)$	[20b]
2128	$[ClC\{C(Me)N(Xyl)\}_2]Cu(CNXyl)$	[20c]
2138	*t*BuNC	[20d]
2148	$[C\{C(Me)N(Mes)\}_2]Cu(CNtBu)$	[20e]
2155	$[HB(Pz)_3]Cu(CNtBu)$	[20f]
2176	$[N\{(C_3F_7)C(Dipp)N\}_2]Cu(CNtBu$	[20e]
2193	**4b**	this work
2196	$[HB(3,5\text{-}(CF_3)_2Pz)_3]Cu(CNtBu)$	[20g]
2199	**4a**	this work
2164/2210	$[(CO)_3Re(pz)_3\{M(CNcHex)\}_2]$	[20h]

The small variance of the Cu–N and N–N bond lengths with values in the range 1.878(2)–1.887(2) Å and 1.302(3)–1.315(3) Å indicates a symmetric bonding situation. With 1.882 Å the average Cu–N distance is almost identical to the corresponding values in the two other structurally characterized copper(I) triazenides $[CuN_3Ph_2]_2$ (1.898(3) Å) [21] and $[CuN_3Dip_2]_2$ (1.8818(16) Å) [22]. The observed Cu1···Cu2 contact distance of 2.4765(5) Å is typical for dimeric copper complexes [23].

3.4.2. Molecular structures of the isonitrile adducts $[Cu\{N_3(Dmp)Tph\}(CNtBu)]$ (**4b**) and **4b**·C_6H_6

Since the structural analysis of the solvent-free complex **4b** is hampered by disorder of the copper atom the following discussion focusses on the molecular structure of the packing complex **4b**·C_6H_6. The complex crystallizes with monomeric units in the monoclinic space group $P2_1/c$ (Fig. 3). The copper atom shows a linear coordination (C1–Cu–N3 = 173.73(5)°) by the Tph-substituted nitrogen atom N3 and the carbon atom C1 of the isonitrile donor. The η^1-coordination of the triazenido ligand is remarkable since similiar isonitrile adducts of copper β-diketiminate always possess an N,N-chelating binding mode [20a,b,c,e].

The higher nucleophilic character of N3 compared to the Dpp-substituted nitrogen atom N1 may be explained by the stronger overlap of the NNN and (C31 → C36)-π-systems as indicated by the different torsion angles N2–N1–C11–C16 [−42.77(17)°] and

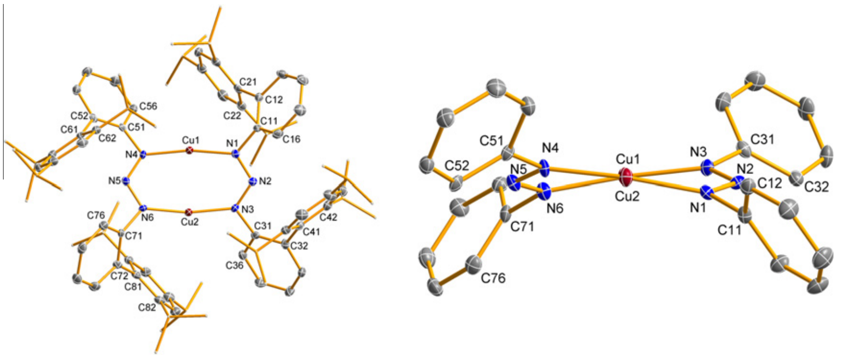

Fig. 2. Molecular structure of dimeric copper triazenide $(\mathbf{2a})_2$ with thermal ellipsoids set to 50% probability. For clarity carbon atoms of iso-propyl groups are reduced in size (left) and carbon atoms of Tph substituents have been omitted (right).

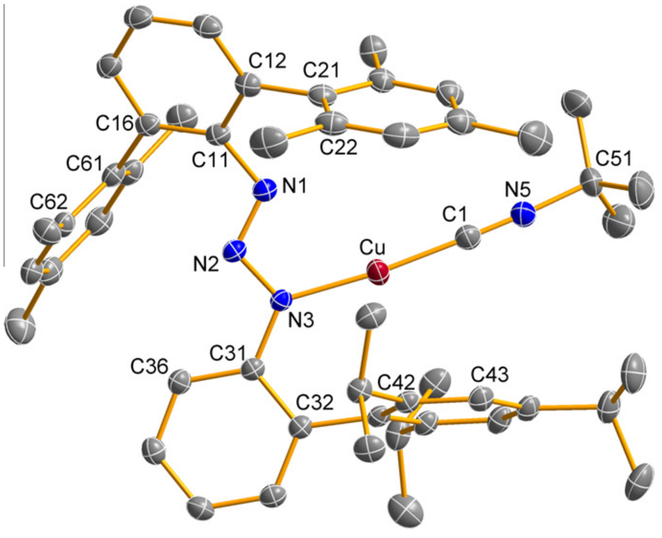

Fig. 3. Molecular structure of the isonitrile adduct $\mathbf{4b}\cdot C_6H_6$ with thermal ellipsoids set to 50% probability. Hydrogen atoms and the cocrystallized solvent have been omitted.

N2–N3–C31–C36 [21.64(17)°]. A smaller torsion angle allows higher transfer of electron density from the π-system of the C_6H_4 ring to the adjacent nitrogen atom. The η^1-coordination of the triazenido ligand accounts for significantly different N–N distances of 1.2816(16) Å (N1–N2) and 1.3354(16) Å (N2–N3). With bond lenghts of 1.8948(12) Å, 1.8337(15) Å, and 1.147(2) Å, respectively, the Cu–N, Cu–C and C≡N distances are almost identical to the corresponding values in the three-nuclear complex $[(CO)_3Re(pz)_3\{Cu(CNcHex)\}_2]$ (1.881(5), 1.834(7) and 1.151(8) Å) [20h] with a structurally related N–Cu–C≡N–R fragment. The copper β-diketiminate $[(C\{C(Me)N(Mes)\}_2)Cu(CNtBu)]$[20e] shows comparable Cu–C and C≡N bond distances of 1.8273(18) Å and 1.154(2) Å but notably longer Cu–N distances of 1.9232(13) Å and 1.9604(14) Å that may be attributed to the chelating coordination mode of the β-diketiminato ligand.

In the molecular structure of the solvate-free isonitrile adduct **4b** disorder of the copper atom is observed. Although refinement with two split positions is possible, the anisotropic displacement parameters indicate a shallow energy profile for the coordination of the metal atom and a high mobility parallel to an imaginary axis through the nitrogen atoms N1 and N3 (Fig. 4). The side occupation factor of the minor site depends on the data collection temperature and increases from 5% at −173 °C to 12% at −100 °C. Contrary to the well ordered structure of $\mathbf{4b}\cdot C_6H_6$ the disorder in **4b** probably arises from small conformational differences due to the cocrystallized solvent. Apparently, the different NNCC torsion angles of −37.3(2)° in **4b** versus −42.77(17)° in $\mathbf{4b}\cdot C_6H_6$ lead to a small but significant increase of the nucleophilicity of nitrogen atom N1.

3.4.3. *Molecular structure of the triphenylphosphane adduct $[Cu\{N_3(Dmp)Tph\}(PPh_3)_2]\cdot C_7H_8$ (**5a**·toluene)*

The monomeric compound crystallizes as packing complex with toluene in the triclinic space group $P\bar{1}$ (Fig. 5). The copper atom possesses a severely distorted tetrahedral coordination with interligand angles in the range 59.06(8)–123.01(6)° by the two η^2-coordinated nitrogen atoms N1 and N3 of the triazenido ligand and the phosphorous atoms P1 and P2 of the two triphenylphosphane donors. In an alternative description that assigns only one

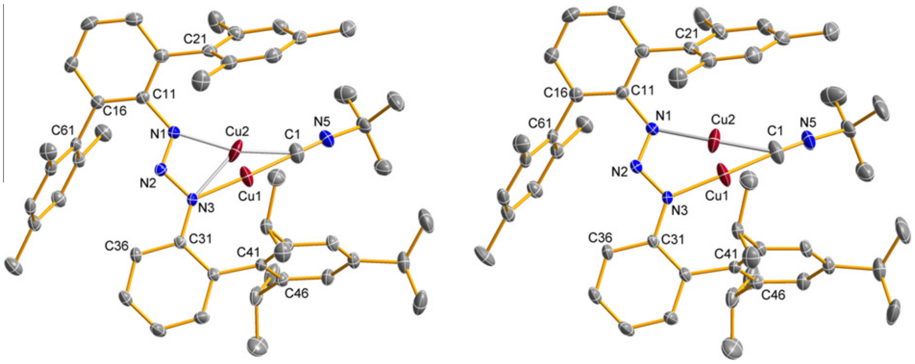

Fig. 4. Molecular structures of the solvate-free isonitrile adduct **4b** at −173 °C (left, ellipsoids with 50% probability) and −100 °C (right, ellipsoids with 30% probability). Hydrogen atoms have been omitted. Side occupation factors for Cu2: 0.05 (−173 °C), 0.12 (−100 °C).

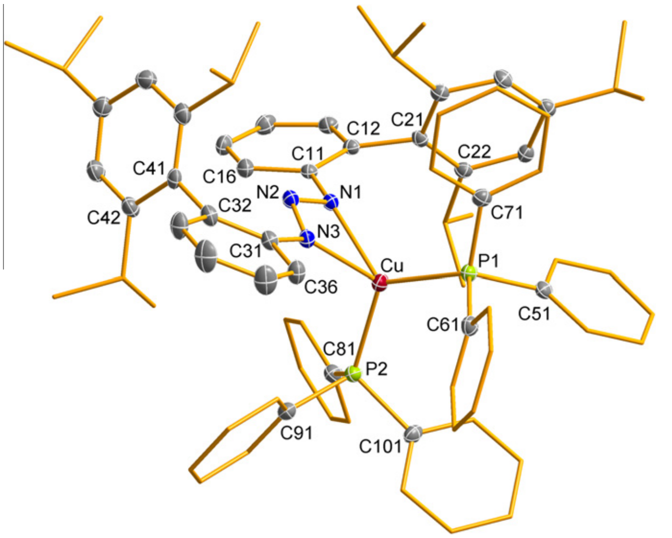

Fig. 5. Molecular structure of the bis(triphenylphosphane) adduct **3a** with thermal ellipsoids set to 30% probability. For clarity carbon atoms of iso-propyl groups and PPh_3 ligands are reduced in size and hydrogen atoms have been omitted.

coordination site, represented by N2, to the small-bite triazenido ligand the copper atom shows a trigonal planar coordination with interligand angles in the range 114.8(5)–122.3(5)°. According to the torsion angles N2–N1–C11–C16 and N2–N3–C31–C36 of −31.2(3)°, respectively −165.8(2)° a syn/anti-conformation of both Tph substituents is realized.

The different Cu–N distances (Cu–N1 2.220(2) Å, Cu–N3 2.117(2) Å) indicate an asymmetric coordination of the triazenido ligand while the coordination of the two triphenylphosphane donors is rather symmetrical (Cu–P1 2.2706(9) Å, Cu–P2 2.2814(9) Å). The average Cu–N distances of 2.169 Å is widened by 0.28 Å compared to the corresponding distances in the η^1-coordinated complexes **2a** and **4b**. In some related PPh_3 complexes, the β-dialdiminate $[\{PhC(C(H)N(Ph))_2\}Cu(PPh_3)_2]$ [24] and the bi-nuclear oxalimidinate $[(Ph_3P)_2Cu\{(Tol)N\}_2CC\{N(Tol)\}_2Cu(PPh_3)_2]$ [25] Cu–N and Cu–P bond lengths of 2.053(3) Å and 2.292(1) Å, respectively 2.063(5) Å and 2.291(2) Å are observed.

4. Conclusion

In summary, we have used sterically crowded, triazenido ligands for the synthesis of monomeric and dimeric copper complexes. The IR spectroscopic characterization of the isonitrile adducts allowed for the first time to experimentally probe the donor character of the triazenido ligands, which are as expected weaker donors than the related β-diketiminato ligands.

Acknowledgements

We thank the Deutsche Forschungsgemeinschaft (SPP 1166) for financial support and Dr. Falk Lissner for the collection of three X-ray data sets.

Appendix A. Supplementary material

CCDC 800783, 800784, 800785, 800786, 800787 and 800788 contain the supplementary crystallographic data for compounds **1a**, (**2a**)$_2$, **3a**·C_7H_8, **4b** (at 100 K), **4b** (at 173 K) and **4b**·C_6H_6, respectively. These data can be obtained free of charge from The Cambridge Crystallographic Data Centre via www.ccdc.cam.ac.uk/data_request/cif. Supplementary data associated with this article can be found, in the online version, at doi:10.1016/j.ica.2011.01.079.

References

[1] V.C. Gibson, S.K. Spitzmesser, Chem. Rev. 103 (2003) 283.
[2] L. Bourget-Merle, M.F. Lappert, J.R. Severn, Chem. Rev. 102 (2002) 3031.
[3] (a) J. Barker, M. Kilner, Coord. Chem. Rev. 133 (1994) 219;
(b) F.T. Edelmann, Adv. Organomet. Chem. 57 (2008) 183.
[4] (a) D.D. Moore, S.D. Robinson, Adv. Inorg. Chem. Radiochem. 30 (1986) 1;
(b) K. Vrieze, G. van Koten, in: G. Wilkinson (Ed.), Comprehensive Coordination Chemistry, vol. 2, Pergamon Press, Oxford, 1987, p. 189.
[5] S.-O. Hauber, F. Lissner, G.B. Deacon, M. Niemeyer, Angew. Chem., Int. Ed. 44 (2005) 5871.
[6] H.S. Lee, M. Niemeyer, Inorg. Chem. 45 (2006) 6126.
[7] S. Balireddi, M. Niemeyer, Acta Crystallogr., Sect. E 63 (2007) o3525.
[8] M. Niemeyer, S.-O. Hauber, Inorg. Chem. 44 (2005) 8644.
[9] H.S. Lee, S.-O. Hauber, D. Vinduš, M. Niemeyer, Inorg. Chem. 47 (2008) 4401.
[10] H. Eriksson, M. Håkansson, Organometallics 16 (1997) 4243.
[11] (a) H. Hope, Progr. Inorg. Chem. 41 (1995) 1;
(b) SHELXTL PC 5.03, Siemens Analytical X-Ray Instruments Inc., Madison, WI, 1994.;
(c) G.M. Sheldrick, SHELXL, Program for Crystal Structure Solution and Refinement, Universität Göttingen, 1997.
[12] S.G. Alexander, M.L. Cole, C.M. Forsyth, S.K. Furfari, K. Konstas, Dalton Trans. (2009) 2326.
[13] S. Patai, Z. Rappoport, The Chemistry of Amidines and Imidates, Wiley, Chichester, 1991.
[14] A.G.M. Barrett, M.R. Crimmin, M.S. Hill, P.B. Hitchcock, G. Kociok-Köhn, P.A. Procopiou, Inorg. Chem. 47 (2008) 7366.
[15] (a) R.M. Anulewicz, Acta Crystallogr., Sect. C 53 (1997) 345;
(b) M. Hörner, I.C. Casagrande, J. Bordinhao, C.M. Mössmer, Acta Crystallogr., Sect. C 58 (2002) o193;
(c) M. Hörner, L. Bresolin, J. Bordinhao, E. Hartmann, J. Strähle, Acta Crystallogr., Sect. C 59 (2003) o426;
(d) N. Karadayi, S. Çakmak, M. Odabaşo, O. Büyükgüngör, Acta Crystallogr., Sect. C 61 (2005) o303.
[16] S.-O. Hauber, J.-W. Seo, M. Niemeyer, Z. Anorg. Allg. Chem. 636 (2010) 750.
[17] H.S. Lee, M. Niemeyer, Unpublished work.
[18] R. Litlabø, H.S. Lee, M. Niemeyer, K.W. Törnroos, R. Anwander, Dalton Trans. 39 (2010) 6815.
[19] H.S. Lee, M. Niemeyer, Inorg. Chem. 49 (2010) 730.
[20] (a) Y.M. Badiei, T.H. Warren, J. Organomet. Chem. 690 (2005) 5989;
(b) B.A. Jazdzewski, P.L. Holland, M. Pink, V.G. Young Jr., D.J.E. Spencer, W.B. Tolman, Inorg. Chem. 40 (2001) 6097;
(c) D.J.E. Spencer, A.M. Reynolds, P.L. Holland, B.A. Jazdzewski, C. Duboc-Toia, L. Le Pape, S. Yokota, Y. Tachi, S. Itoh, W.B. Tolman, Inorg. Chem. 41 (2002) 6307;
(d) H.V.R. Dias, S. Singh, Inorg. Chem. 43 (2004) 5786;
(e) Y.M. Badiei, A. Krishnaswamy, M.M. Melzer, T.H. Warren, J. Am. Chem. Soc. 128 (2006) 15056;
(f) M. I Bruce, A.P.P. Ostazewski, J. Chem. Soc., Dalton Trans. (1973) 2433;
(g) H.V.R. Dias, H.-L. Lu, J.D. Gorden, W. Jin, Inorg. Chem. 35 (1996) 2149;
(h) G.A. Ardizzoia, G. La Monica, A. Maspero, N. Masciocchi, M. Moret, Eur. J. Inorg. Chem. (1999) 1301.
[21] L.R. Falvello, E.P. Urriolabeitia, U. Mukhopadhyay, D. Ray, Acta Crystallogr., Sect. C 55 (1999) 170.
[22] A.L. Johnson, A.M. Willcocks, S.P. Richards, Inorg. Chem. 48 (2009) 8613.
[23] H.L. Hermann, G. Boche, P. Schwerdtfeger, Chem. Eur. J. 7 (2001) 5333.
[24] X. Li, J. Ding, W. Jin, Y. Cheng, Inorg. Chim. Acta 362 (2009) 233.
[25] L. Böttcher, D. Walther, H. Görls, Z. Anorg. Allg. Chem. 629 (2003) 1208.